MnSe phase segregation during heteroepitaxy of Mn doped Ga_2Se_3 on Si(001)

T. C. Lovejoy,[1,a] E. N. Yitamben,[1] S. M. Heald,[2] F. S. Ohuchi,[3] and M. A. Olmstead[1]
[1]*Department of Physics, University of Washington (UW), Box 351560, Seattle, Washington 98195, USA and Center for Nanotechnology (CNT), UW, Seattle, Washington 98195, USA*
[2]*Advanced Photon Source, Argonne National Lab, Argonne, Illinois 60439, USA*
[3]*Department of Materials Science and Engineering, UW, Box 352120, Seattle, Washington 98195, USA and CNT, UW, Seattle, Washington 98195, USA*

(Received 19 September 2009; accepted 21 November 2009; published online 17 December 2009)

Heteroepitaxial thin films of Mn-doped Ga_2Se_3 are grown by molecular beam epitaxy on Si(001):As. Mn-doped films are laminar for the first 1–2 nm, after which oriented islands with flat tops are observed by scanning tunneling microscopy. In contrast with the bulk phase diagram, which predicts $MnGa_2Se_4$ precipitates, the precipitates are identified by bond length measurements from extended x-ray absorption fine structure as rocksalt MnSe. This difference is attributed to superior lattice matching of MnSe to the substrate, and an epitaxial relationship between the MnSe and Si substrate is inferred. © *2009 American Institute of Physics*. [doi:10.1063/1.3273858]

Transition metal (TM) doping of semiconductors leads to a variety of interesting (and useful) optical, magnetic, and electronic properties. Extensive effort has been expended in exploring TM-doped dilute magnetic semiconductor (DMS) materials with a goal of developing a room-temperature, silicon-compatible ferromagnet.[1] A key issue in this quest is solubility of the TM in the semiconductor host.[2,3] To maximize the Curie temperature and prevent the formation of MnAs clusters in the prototype DMS, Mn-doped GaAs, low temperature growth techniques,[4] coupled with elaborate post-growth annealing schemes have been developed.[5] However, Mn has a high solubility in bulk Ga_2Se_3,[6] and the close similarity between GaAs and Ga_2Se_3 suggests that Mn-doping of the latter could lead to an equally interesting DMS as Mn-doped GaAs. Very close lattice matching ($\sim$0.1%) allows for high quality epitaxy of Ga_2Se_3 on technologically ubiquitous Si,[7] and theoretical calculations predict that Mn-doped Ga_2Se_3 should be ferromagnetic, at least at $T=0$ K.[8] These make it an intriguing candidate for exploration as a DMS.

Ga_2Se_3 is related to GaAs by the addition of one proton and one valence electron at each anion site, and the removal of one in every three cations, including its three valence electrons. These intrinsic cation vacancies maintain charge neutrality within the crystal. Relative to GaAs there are distortions in the atomic positions and changes in the electronic structure related to the vacancies.[9,10] With respect to transition metal doping, Ga_2Se_3 is more complex than GaAs because the number of likely dopant sites must be increased to include the vacant sites.[11]

The bulk phase diagram of MnSe-Ga_2Se_3 has been reported based on x-ray diffraction.[6] As the Mn concentration is increased, a single phase similar to undoped Ga_2Se_3 ($a=5.43$ Å) with "apparent cubic zinc blende form" and increasing lattice constant was observed up to 6 at. % Mn. A secondary phase of the nearly zinc-blende $MnGa_2Se_4$ ($a=5.86$ Å) appeared at 9 at. %. With increasing Mn, after a small window of pure $MnGa_2Se_4$, a second phase of rocksalt MnSe ($a=5.44$ Å) appeared at 16 at. %. While neither exhibit ferromagnetism, MnSe and $MnGa_2Se_4$ have very different magnetic phase diagrams. $MnGa_2Se_4$ is antiferromagnetic below 8 K.[12] The MnSe case is more complicated, with structural transitions occurring simultaneously with magnetic transitions to antiferromagnetism between 90 and 300 K.[13] The unusual temperature dependence of the magnetization in Mn doped layered GaSe [Ref. 14] is a subject of recent interest[15] due to the possibility of a *re-entrant* carrier-mediated ferromagnetic semiconductor, which becomes ferromagnetic as temperature is *increased* due the increase in free carrier density. This raises the question of what the magnetic behavior of low concentration Mn substituting in the nearly zinc-blende Ga_2Se_3 might be. An essential first step toward possible DMS application of Mn:Ga_2Se_3 is mapping its solubility properties in thin film growth.

In this letter, we use direct real space imaging to study the Mn-doping of Ga_2Se_3 and subsequent phase segregation. Thin films of Mn doped Ga_2Se_3 grown with molecular beam epitaxy (MBE) on Si(001):As are studied with scanning tunneling microscopy (STM) and extended x-ray absorption fine structure (EXAFS). In the dilute and thin limit, laminar Mn-doped films are observed, but before films are thick or concentrated enough to be of interest for magnetism studies, phase segregation is observed. For thicker or higher Mn concentration films, low, wide islands are observed by STM. The islands have flat tops with edges highly aligned along the [110] and [1$\bar{1}$0] substrate directions. In apparent contradiction with the bulk phase diagram, the observed islands are identified by bond length measurements from EXAFS as precipitates of the rocksalt compound MnSe. Better lattice matching to the substrate for two phase Ga_2Se_3+MnSe is used to explain the difference from the bulk case, and an epitaxial relationship between the MnSe and Ga_2Se_3/Si substrate is proposed.

Preparation of quality undoped Ga_2Se_3 films by MBE on clean, arsenic terminated, Si(001) substrates is addressed elsewhere.[7] Evaporation from a GaSe source onto a hot Si(001):As substrate (450–500 °C) at flux rates of 4–8 Å/min results in a laminar, epitaxial Ga_2Se_3 film. These parameters are held fixed for the doping experiments. Mn is

[a]Electronic mail: tlovejoy@u.washington.edu.

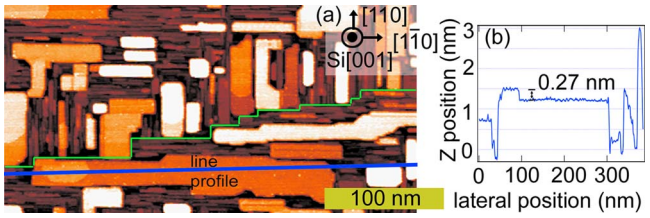

FIG. 1. (Color online) (a) STM image of Mn doped Ga_2Se_3 film grown on Si(001):As. Many ~2 nm tall, 10–250 nm wide islands are observed with highly aligned edges. The green zig-zag line highlights a substrate step edge. (V_{tip}=−3 V,0.1 nA) (b) Line profile along blue line in (a) showing 2.7 Å step height of incomplete island layers.

dosed by separate Knudsen cell. Film dosing and Mn concentration are determined by separately calibrating the incident Mn and GaSe fluxes with a water cooled quartz crystal monitor and measuring the deposition time. The amount of material in the film is lower than the exposure dose due to re-evaporation during growth on hot substrate, which can be as large as ~70% in the undoped case.[16] After growth, films are transferred in ultrahigh-vacuum (UHV) for measurement with a commercial (Omicron) UHV-STM and x-ray photoelectron spectroscopy (XPS). There is an oxygen peak in the XPS spectra only after exposure to air, which suggests that the films oxidize somewhat upon exposure to atmosphere. The STM (EXAFS) data shown in Figs. 1 and 2 is from a film dosed with 3 nm (3 nm) pure Ga_2Se_3, followed by codeposition of 3 nm (10 nm) Ga_2Se_3 and 0.25 nm (1 nm) Mn.

Samples grown and checked in UHV with STM and XPS were transported through, and measured in, air for EXAFS measurements at the Advanced Photon Source sector 20BM PNC/XOR-CAT. Samples were mounted on spinners and rotated about the sample normal at about 3 Hz during measurement where x-rays polarized near the plane of the sample impinged at grazing incidence (2°–3°). The x-ray energy was scanned through the Ga (not shown), Se, and Mn K-edge energies, and the K-edge fluorescence was captured from near the plane of the sample (~5°) with a liquid nitrogen cooled, thirteen element Ge detector.

STM studies of a series Mn-doped films reveal that for low Mn concentrations (<6 at. %) and small dosing (<5 nm) laminar films with morphology similar to that reported[7] for pure Ga_2Se_3 are observed. Islands are observed in films with higher dosing or higher Mn concentration. For example, 5 nm Ga_2Se_3 codeposited with 0.05 nm Mn (~1 at. %) results in a laminar film with a thickness deduced from XPS of 3.4 nm, while 10 nm Ga_2Se_3 codeposited

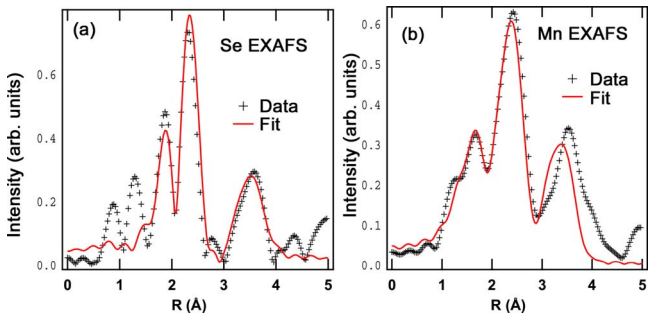

FIG. 2. (Color online) Magnitude of the Fourier transform of the k^2-weighted EXAFS spectrum (black crosses) and fit from FEFF computer program (red line) for (a) Se and (b) Mn. The data are well fit assuming Se in MnSe and Ga_2Se_3, with Mn in MnSe and MnO.

with 0.17 nm Mn (~2 at. %) results in an islanded film. For higher Mn concentration (~10 at. %), islands are observed in relatively thin films (~1 nm). The film and island morphology also depends on post-growth annealing, and the presence or absence of undoped buffer layers in a complicated and interesting way. This paper only addresses the case where an undoped Ga_2Se_3 epitaxial layer is followed by a Mn doped layer. The effect of other growth conditions on the island morphology will be reported in a separate publication.[10]

Figure 1(a) shows a characteristic island morphology for a Mn doped Ga_2Se_3 film with ~8 at. % Mn. About 50% of the surface is covered with islands whose edges are highly aligned along the [110] and [1$\bar{1}$0] substrate directions. Typical island heights range from 1–3 nm, while the island widths exhibit a much wider distribution, from 10–250 nm. Each island is elongated in one direction such that one dimension is between 2 and 10 times longer than the other.

As with the dimer rows of the substrate, the long direction of the film and island morphology rotate 90° at each substrate step. This makes the substrate steps clearly identifiable in Fig. 1(a); one such step is highlighted by the green zig-zag line. The islands are mostly confined to single terraces and usually do not cross substrate steps. This causes the islands on some terraces to be longer than others, i.e., the longer islands are parallel to step edges.

Several islands have an incomplete top layer—covering 10%–90% of the island. The step height of this layer can be seen in Fig. 1(b), which shows a line profile through Fig. 1(a). In each case the layer height is 2.7 ± 0.1 Å.

The local bonding environment of each elemental constituent of the film may be extracted from K-edge EXAFS. Figure 2 shows the magnitude of the k^2-weighted Se (a) and Mn (b) EXAFS Fourier transform as a function of radial distance from the atom. In both cases the peaks between 1.5 and 2.5 Å correspond roughly to the first neighbor bond lengths, and the peaks between 3 and 4 Å to the second neighbor bonds. A simultaneous fit of the Mn and Se data using a simulation from the FEFF computer program to the EXAFS spectra over a k range of 2–12.95 $Å^{-1}$ and R range of 1.4–4 Å was used to determine the bond lengths. For the FEFF simulation, the Se was assumed to be either in Ga_2Se_3 or MnSe, while the Mn was assumed in either MnSe or MnO. First and second neighbors were included from MnSe and Ga_2Se_3 while only first neighbors were included from MnO. The second neighbor bond lengths were constrained to their ideal values based on the first neighbor bond length in the given structure. The fit had 15 variables, compared to the spectra which together have about 37 independent points. The results of the fit are shown in red in Figs. 2(a) and 2(b). The best-fit first neighbor bond lengths are 2.14 ± 0.03 Å for the Mn–O, 2.71 ± 0.01 Å for Mn–Se or Se–Mn, and 2.39 ± 0.01 Å for Se–Ga. We also observed the 2.39 Å bond length for Se in undoped films (not shown), which is close to the literature value for Ga_2Se_3 (2.43 Å).[17]

Under equilibrium bulk crystal growth, Mn–Ga–Se disproportionates at these Mn concentrations into Mn-doped Ga_2Se_3 and $MnGa_2Se_4$. However, the measured bond lengths in these thin films (2.71 ± 0.01 Å) is not consistent with either the Mn-Se bond length in $MnGa_2Se_4$ (2.55 Å) (Ref. 18) or that expected from Mn substitution on a Ga site (the same as Ga-Se, 2.39 Å). Rather, the EXAFS is consistent

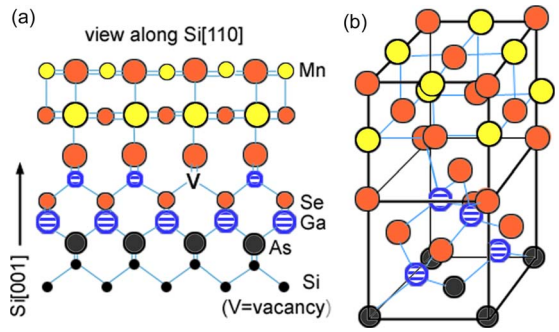

FIG. 3. (Color online) Schematic diagram showing proposed epitaxial relationship between Ga_2Se_3 film and MnSe islands along [110] (a) and in three-dimensional perspective view (b). The Se fcc sublattice continues across the interface.

with rocksalt MnSe (bondlength=$a/2$=2.72 Å). The second neighbor Mn and Se peaks are also well fit by assuming MnSe. Another very short Mn bond is observed (2.14 Å); this corresponds to manganese oxide, which is most likely a result of surface oxidation during atmospheric exposure. The bond length corresponding to Ga_2Se_3 is still observed for Se (2.39 Å) after Mn doping. We thus propose that Se participates in both Ga_2Se_3 and MnSe, while the Mn participates only in MnSe and a surface oxide. Even so, the possibility of a relatively small amount (<5%) of the Mn remaining doped in the Ga_2Se_3 layer cannot be excluded.

Based on the shape and orientation of the islands observed with STM, we propose that the face-centered-cubic (fcc) rocksalt MnSe has an epitaxial relationship with the fcc zinc-blende Ga_2Se_3 underlayer and substrate such that the Se fcc sub-lattice continues across the interface. The step height of the incomplete island layer in Fig. 1(b) (2.7 Å) is indistinguishable from the Mn–Se bond length from EXAFS. This suggests that the Mn–Se bond is oriented perpendicular to the surface, or that the MnSe(001) and Si(001) planes are aligned. It is also apparent from Fig. 1(a) that the MnSe island edges are highly aligned in the plane, implying a specific rotational orientation as well. The MnSe and Ga_2Se_3 lattices both contain a Se fcc sublattice with nearly identical lattice constant. The cation fcc sublattice consists of Mn in the former, and Ga with vacant sites in the latter. In the proposed epitaxial relationship, which is shown in Fig. 3, the cation fcc sublattice changes its composition and displacement vector from the anion sublattice at the interface, but the Se sublattice is unchanged. For this epitaxial relationship, the island edges correspond to (110) facets of MnSe.

The formation of MnSe makes a surprisingly close analogy to the well-known formation of MnAs precipitates in Mn doped GaAs.[2] Though MnAs can be useful as a ferromagnetic material for spin manipulation,[19] typically, efforts are made to prevent the formation of the more thermodynamically favorable MnAs in Mn-doped GaAs by low-temperature (LT)-MBE techniques.[2] When using GaSe source material, as was done here, we find LT-MBE (below about 450 °C) (Ref. 16) causes the formation of layered GaSe instead of Ga_2Se_3. Further development of LT-MBE, with either additional Se or separate Se and Ga sources, should be explored.

We propose that the superior lattice matching of MnSe (a=5.44 Å) to Ga_2Se_3 and Si (5.43 Å) compared to $MnGa_2Se_4$ (5.86 Å) is the reason MnSe forms instead of $MnGa_2Se_4$ during heteroepitaxy. The lattice constant of Ga_2Se_3 gradually increases with Mn concentration from within 0.1% of that of Si to about 0.6% at the point where bulk $MnGa_2Se_4$ precipitation occurs (9 at. % Mn). MnSe is intermediate between these end points with ~0.2% lattice mismatch. It is possible that the rigid Si substrate constrains the Mn-doped Ga_2Se_3 lattice, causing the formation of MnSe precipitates for relatively thick films even in the dilute limit. It is reasonable to assume heteroepitaxy of $MnGa_2Se_4$, with its large lattice mismatch of almost 8%, is strongly suppressed relative to MnSe.

In conclusion, phase segregation of MBE grown Mn doped Ga_2Se_3 on Si(001):As has been studied with STM and EXAFS, and shows similarity to the prototype dilute magnetic semiconductor Mn doped GaAs. Islands observed with STM are identified by Mn-Se bond length measurements from EXAFS as the rocksalt compound MnSe. This is in apparent contradiction with the bulk phase diagram that suggests $MnGa_2Se_4$ should form, but closer lattice matching of MnSe to the substrate can account for this difference. Based on the highly oriented island morphology, incomplete layer heights, and similarity in crystal structure and lattice constant, the authors speculate that the epitaxial relationship between the MnSe and Ga_2Se_3 leaves the Se fcc sublattice unperturbed at the interface.

This work was supported by the NSF (Grant No. DMR-0605601). Use of the Advanced Photon Source is supported by the DOE under Contract No. DE-AC02-06CH11357. T.C.L. and E.N.Y. acknowledge fellowship support: T.C.L.-IGERT Fellowship No. NSF/NCI DGE 0504573 through the Center for Nanotechnology at the UW, E.N.Y.-IBM Fellowship.

[1] S. Wolf, D. Awschalom, R. Buhrman, J. Daughton, S. Von Molnar, M. Roukes, A. Chtchelkanova, and D. Treger, Science **294**, 1488 (2001).
[2] H. Ohno, Science **281**, 951 (1998).
[3] A. MacDonald, P. Schiffer, and N. Samarth, Nature Mater. **4**, 195 (2005).
[4] H. Ohno, A. Shen, F. Matsukura, A. Oiwa, A. Endo, S. Katsumoto, and Y. Iye, Appl. Phys. Lett. **69**, 363 (1996).
[5] S. J. Potashnik, K. C. Ku, S. H. Chun, J. J. Berry, N. Samarth, and P. Schiffer, Appl. Phys. Lett. **79**, 1495 (2001).
[6] M. Morocoima, M. Quintero and J. C. Woolley, Phys. Status Solidi A **141**, 53 (1994).
[7] T. Ohta, D. A. Schmidt, S. Meng, A. Klust, A. Bostwick, Q. Yu, M. A. Olmstead, and F. S. Ohuchi, Phys. Rev. Lett. **94**, 116102 (2005).
[8] N. wa Gatuna, Ph.D. thesis, University of Washington, 2007.
[9] M. Peressi and A. Baldereschi, J. Appl. Phys. **83**, 3092 (1998).
[10] T. C. Lovejoy, E. N. Yitamben, S. M. Heald, T. Ohta, J. Morales, F. S. Ohuchi, and M. A. Olmstead (unpublished).
[11] E. N. Yitamben, T. C. Lovejoy, D. F. Paul, J. B. Callaghan, F. S. Ohuchi, and M. A. Olmstead, Phys. Rev. B **80**, 075314 (2009).
[12] M. Morocoima, M. Quintero, E. Quintero, J. González, R. Tovar, P. Bocaranda, J. Ruiz, N. Marchán, D. Caldera, E. Calderon, J. C. Woolley, G. Lamarche, A.-M. Lamarche, J. M. Broto, H. Rakoto, L. D'Onofrio, and R. Cadenas, J. Appl. Phys. **100**, 053907 (2006).
[13] Z. V. Popović and A. Milutinović, Phys. Rev. B **73**, 155203 (2006).
[14] T. M. Pekarek, B. C. Crooker, I. Miotkowski, and A. K. Ramdas, J. Appl. Phys. **83**, 6557 (1998).
[15] A. G. Petukhov, I. Žutić, and S. C. Erwin, Phys. Rev. Lett. **99**, 257202 (2007).
[16] T. Ohta, Ph.D. thesis, University of Washington, 2004.
[17] S. Takatani, A. Nakano, K. Ogata, and T. Kikawa, Jpn. J. Appl. Phys., Part 2 **31**, L458 (1992).
[18] M. Cannas, L. Garbato, A. Geddo Lehmann, N. Lampis, and F. Ledda, Cryst. Res. Technol. **33**, 417 (1998).
[19] P. Hai, S. Ohya, M. Tanaka, S. Barnes, and S. Maekawa, Nature (London) **458**, 489 (2009).